Anomalous Hall effect with giant hysteresis loop in $La_{0.67}Sr_{0.33}MnO_3|SrRuO_3$ superlattices

Y. Shiomi,[1,2] Y. Handa,[1] T. Kikkawa,[1,3] and E. Saitoh[1,2,3,4]

[1]*Institute for Materials Research, Tohoku University, Sendai 980-8577, Japan*
[2]*Spin Quantum Rectification Project, ERATO, Japan Science and Technology Agency, Aoba-ku, Sendai 980-8577, Japan*
[3]*WPI Advanced Institute for Materials Research, Tohoku University, Sendai 980-8577, Japan*
[4]*Advanced Science Research Center, Japan Atomic Energy Agency, Tokai 319-1195, Japan*

(Received 5 June 2015; published 16 July 2015)

We report anomalous Hall effects exhibiting a hysteresis loop as large as about 10 T in a ferromagnetic superlattice comprising $La_{0.67}Sr_{0.33}MnO_3$ and $SrRuO_3$ layers. The superlattices grown by pulsed laser deposition exhibit a strong antiferromagnetic interlayer coupling below 110 K, where both $La_{0.67}Sr_{0.33}MnO_3$ and $SrRuO_3$ layers show anomalous Hall effects. With increasing magnetic-field strength, the anomalous Hall resistivity in the superlattices changes its sign depending on the magnetization directions of the $La_{0.67}Sr_{0.33}MnO_3$ and $SrRuO_3$ layers. As a consequence of competition among the antiferromagnetic interlayer coupling, the Zeeman effect, and magnetic anisotropies, the width of the hysteresis loop in the anomalous Hall resistivity in the superlattices becomes larger than 8 T at 10 K, clearly greater than those observed in $La_{0.67}Sr_{0.33}MnO_3$ and $SrRuO_3$ single layer films.

DOI: 10.1103/PhysRevB.92.024418 PACS number(s): 75.47.−m, 73.50.Jt, 75.70.−i

I. INTRODUCTION

Anomalous Hall effects are one of the fundamental and typical spin-dependent transport phenomena in ferromagnets [1]. While normal Hall effects are caused by Lorentz forces, the origin of anomalous Hall effects is the spin-orbit interaction, which connects spin polarizations with orbital motions of conduction electrons. A full understanding of the physical mechanism of anomalous Hall effects has long been challenging, and many studies have been conducted for various ferromagnetic conductors [1].

Hall effects are characterized by the Hall resistivity, $\rho_{yx} = (V_H/I)t$, where V_H is the Hall voltage generating along the y axis, I is the electric current applied along the x axis, and t is the sample thickness [see Fig. 1(a)]. The Hall resistivity in ferromagnetic conductors consists of normal and anomalous Hall resistivities. Namely, ρ_{yx} is described by the relation

$$\rho_{yx} = R_0\mu_0 H + R_s M, \tag{1}$$

with H and M being the magnetic field and the magnetization along the direction perpendicular to the sample (z axis), respectively. R_0 is the normal Hall coefficient, while R_s is the anomalous Hall coefficient. Since the magnitude of the anomalous Hall resistivity ($R_s M$) is usually greater than that of the normal Hall one ($R_0\mu_0 H$) in a low-H range, ρ_{yx} in ferromagnets is usually proportional to the magnetization.

In the present paper, we have investigated the anomalous Hall effect in a ferromagnetic superlattice comprising $La_{0.67}Sr_{0.33}MnO_3$ and $SrRuO_3$ layers. $La_{0.67}Sr_{0.33}MnO_3$ and $SrRuO_3$ are ferromagnetic metals, but their magnetic properties are different; bulk $La_{0.67}Sr_{0.33}MnO_3$ is a soft ferromagnet with a high $T_C \approx 350$ K and a moment of $\sim 3.5\mu_B$/Mn, while bulk $SrRuO_3$ is a hard ferromagnet with a low $T_C \approx 150$ K and $\sim 1.5\mu_B$/Ru. Although the anomalous Hall effects in $La_{0.67}Sr_{0.33}MnO_3$ and $SrRuO_3$ have been investigated well so far [2–12], the anomalous Hall effect in hybrid structures made of the two ferromagnetic metals is an intriguing issue.

Importantly, magnetizations of the $La_{0.67}Sr_{0.33}MnO_3$ and $SrRuO_3$ layers are known to be coupled antiferromagnetically to each other [13–20], which should affect the anomalous Hall effect in $La_{0.67}Sr_{0.33}MnO_3|SrRuO_3$ multilayer systems. The interfacial antiferromagnetic coupling between $La_{0.67}Sr_{0.33}MnO_3$ and $SrRuO_3$ layers [13–21] has been attributed to the hybridization of $2p$ states of O atoms with $3d$ states of Mn atoms and $4d$ states of Ru atoms [13,14]. The antiferromagnetic interlayer coupling associates the magnetization process of $La_{0.67}Sr_{0.33}MnO_3$ layers with that of $SrRuO_3$ layers, and thus will affect the anomalous Hall effect in $La_{0.67}Sr_{0.33}MnO_3|SrRuO_3$ superlattices. In fact, here we observe a very large hysteresis loop of $\sim$10 T in the Hall resistivity in $La_{0.67}Sr_{0.33}MnO_3|SrRuO_3$ superlattice samples at 10 K, which is produced by magnetic competition among the antiferromagnetic interlayer coupling, the Zeeman effect driven by an external magnetic field, and the magnetic anisotropies of $SrRuO_3$ layers developing at low temperatures.

II. METHODS

$La_{0.67}Sr_{0.33}MnO_3|SrRuO_3$ superlattice samples were grown by pulsed laser deposition using a KrF excimer laser on $SrTiO_3$ (001) substrates at 800 °C in 0.3 Torr O_2 [22]. After deposition, samples were annealed at 800 °C in the 400 Torr O_2 atmosphere for 1 h and then cooled to room temperature. The fabricated superlattices consist of ten periods of a $La_{0.67}Sr_{0.33}MnO_3$ layer and a $SrRuO_3$ layer. The superlattice structure was confirmed by transmission electron microscopy (TEM), as shown in Figs. 1(b) and 1(c). From the TEM measurements, the thicknesses of the $La_{0.67}Sr_{0.33}MnO_3$ and $SrRuO_3$ layers are estimated to be 2.4 and 3.5 nm, respectively [Fig. 1(c)]. The total thickness of the superlattice sample is about 57 nm. The longitudinal resistivity, Hall resistivity, and magnetization for the superlattice samples were measured in a Physical Property Measurement System (Quantum Design, Inc.), where an external magnetic field was applied perpendicular to the superlattices (i.e., parallel to the z axis). For reference, the magnetization of a $SrTiO_3$ substrate was measured in the same experimental condition; the substrate

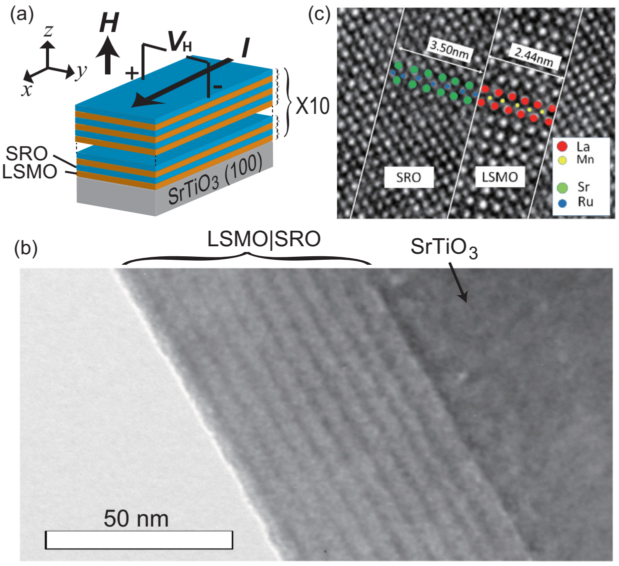

FIG. 1. (Color online) (a) A schematic illustration of the Hall effect measurement for a $La_{0.67}Sr_{0.33}MnO_3|SrRuO_3$ superlattice sample. LSMO and SRO denote $La_{0.67}Sr_{0.33}MnO_3$ and $SrRuO_3$ layers, respectively. (b) An overview cross-sectional TEM image for a superlattice sample. A magnified view is shown in (c).

magnetization was subtracted from the magnetization data for superlattice samples.

III. RESULTS AND DISCUSSION

Figure 2(a) shows the temperature (T) dependence of resistivity ρ_{xx} for a representative superlattice sample. In the entire T region below 300 K, ρ_{xx} shows a metallic T dependence ($d\rho_{xx}/dT > 0$). ρ_{xx} at the lowest T is 0.4 mΩ cm, which is almost the same as that of similar superlattices [23]. The residual resistance ratio is larger than 2.

Magnetization M measured under $\mu_0 H = 1$ T in a direction perpendicular to a superlattice sample is shown as a function of T in Fig. 2(b). Here, the diamagnetic contribution of the $SrTiO_3$ substrate was subtracted from the raw data. When T decreases, M increases rapidly below $\sim$300 K, which is assigned to the ferromagnetic transition of $La_{0.67}Sr_{0.33}MnO_3$ layers. M monotonically increases with decreasing T below 300 K, but below 110 K, where $SrRuO_3$ layers exhibit a ferromagnetic transition, a clear decrease in M is observed. This is evidence that the magnetization for the $SrRuO_3$ layers antiferromagnetically couples to that for the $La_{0.67}Sr_{0.33}MnO_3$ layers.

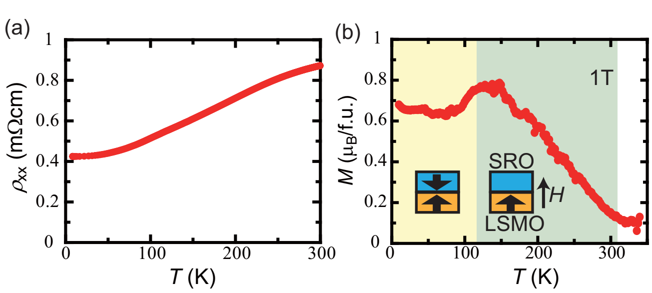

FIG. 2. (Color online) (a) Temperature (T) dependence of resistivity (ρ_{xx}) for a $La_{0.67}Sr_{0.33}MnO_3|SrRuO_3$ superlattice sample. (b) Temperature (T) dependence of magnetization (M) for a $La_{0.67}Sr_{0.33}MnO_3|SrRuO_3$ superlattice sample. The magnetization was measured in a magnetic field of 1 T applied perpendicular to the film plane.

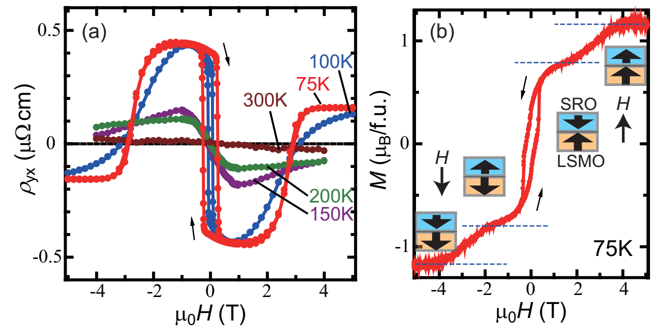

FIG. 3. (Color online) (a) Magnetic-field (H) dependence of Hall resistivity (ρ_{yx}) for a $La_{0.67}Sr_{0.33}MnO_3|SrRuO_3$ superlattice sample at some temperatures below 300 K. (b) Magnetic-field (H) dependence of magnetization (M) at 75 K. The dotted lines are just guides for the eyes. Here, the diamagnetic contribution of the $SrTiO_3$ substrate was subtracted from the raw data.

Figure 3(a) shows the magnetic-field (H) dependence of the Hall resistivity (ρ_{yx}) for a superlattice sample at various temperatures below 300 K. With decreasing T below 300 K, the magnitude of ρ_{yx} increases. ρ_{yx} shows a kink structure around ± 1 T at 200 and 150 K, corresponding to the magnetization saturation field of the $La_{0.67}Sr_{0.33}MnO_3$ layers. In this T range from 300 to 150 K, the $SrRuO_3$ layers are paramagnetic, and only the $La_{0.67}Sr_{0.33}MnO_3$ layers show an anomalous Hall effect. As shown in Fig. 3(a), the sign of the anomalous Hall resistivity is negative in a positive magnetic field, which is consistent with that for $La_{0.67}Sr_{0.33}MnO_3$ single layer films [23].

As T decreases below 110 K, the $SrRuO_3$ layers also show ferromagnetism. At 100 and 75 K, where both $La_{0.67}Sr_{0.33}MnO_3$ and $SrRuO_3$ layers are ferromagnetic, a nonmonotonic H dependence of ρ_{yx} is observed in Fig. 3(a); ρ_{yx} shows the anomalous Hall effect of a negative sign in a low-H regime, while it becomes positive in a high-H range. This sign change around ± 3 T is caused by the anomalous Hall effect in the $SrRuO_3$ layers. The positive sign of anomalous Hall resistivity for the $SrRuO_3$ layers in positive magnetic fields is consistent with the anomalous Hall effect in very thin $SrRuO_3$ films grown on $SrTiO_3$ (001) substrates [11,12]. Hence, the complex H dependence of ρ_{yx} at 100 and 75 K is caused by two anomalous Hall contributions from the $La_{0.67}Sr_{0.33}MnO_3$ and the $SrRuO_3$ layers, where the anomalous coefficients have different signs between the $La_{0.67}Sr_{0.33}MnO_3$ and the $SrRuO_3$ layers.

The H dependence of ρ_{yx} observed at 100 and 75 K [Fig. 3(a)] can be explained by a sum of anomalous Hall contributions from $La_{0.67}Sr_{0.33}MnO_3$ and $SrRuO_3$ layers,

$$\rho_{yx} = \alpha\left(R_0^{\rm LSMO}\mu_0 H + R_s^{\rm LSMO} M^{\rm LSMO}\right) + \beta\left(R_0^{\rm SRO}\mu_0 H + R_s^{\rm SRO} M^{\rm SRO}\right), \qquad (2)$$

where R_0^{LSMO} (R_0^{SRO}), R_s^{LSMO} (R_s^{SRO}), and M^{LSMO} (M^{SRO}) are normal and anomalous Hall coefficients and magnetization for $La_{0.67}Sr_{0.33}MnO_3$ ($SrRuO_3$) layers, respectively. Because of shunting of the electric current inside the superlattices, prefactors α and β are required. In an equivalent circuit model [24], α and β are expressed using resistivities and thicknesses of the $La_{0.67}Sr_{0.33}MnO_3$ and $SrRuO_3$ layers: $\alpha = \rho_{\mathrm{SRO}}^2 t_{\mathrm{LSMO}} t/(\rho_{\mathrm{SRO}} t_{\mathrm{LSMO}} + \rho_{\mathrm{LSMO}} t_{\mathrm{SRO}})^2$ and $\beta = \rho_{\mathrm{LSMO}}^2 t_{\mathrm{SRO}} t/(\rho_{\mathrm{SRO}} t_{\mathrm{LSMO}} + \rho_{\mathrm{LSMO}} t_{\mathrm{SRO}})^2$. Since resistivities in low temperature region below 100 K and thicknesses have similar magnitudes between the $La_{0.67}Sr_{0.33}MnO_3$ and $SrRuO_3$ layers, respectively, $\alpha \sim \beta$ in the present case. R_s^{LSMO} and R_s^{SRO} are constants of negative and positive signs, respectively; ρ_{yx} depends strongly on the magnetization directions of the $La_{0.67}Sr_{0.33}MnO_3$ and $SrRuO_3$ layers.

To examine the magnetization processes of the $La_{0.67}Sr_{0.33}MnO_3$ and $SrRuO_3$ layers under an external magnetic field applied perpendicular to the superlattice, we present in Fig. 3(b) the isothermal magnetization curve for a superlattice at 75 K. At high magnetic fields above ±4 T, since the Zeeman energy overwhelms the energy of the antiferromagnetic interlayer coupling, the magnetizations of the $La_{0.67}Sr_{0.33}MnO_3$ and the $SrRuO_3$ layers ferromagnetically align along the magnetic-field direction ($M^{\mathrm{LSMO}}||M^{\mathrm{SRO}}$). In a low-$H$ range below ∼2 T, however, the strength of the antiferromagnetic coupling at the interface exceeds that of the Zeeman effect, and thus the magnetization of $SrRuO_3$ layers flips to the antiferromagnetic direction ($M^{\mathrm{SRO}} \rightarrow -M^{\mathrm{SRO}}$), as illustrated in Fig. 3(b). This magnetization flip in the $SrRuO_3$ layers at ∼3 T induces the sign reversal of the anomalous Hall contribution from the $SrRuO_3$ layers ($R_s^{\mathrm{SRO}} M^{\mathrm{SRO}} \rightarrow -R_s^{\mathrm{SRO}} M^{\mathrm{SRO}}$). Since the magnitude of the anomalous Hall resistivity for the $SrRuO_3$ layers is greater than that for the $La_{0.67}Sr_{0.33}MnO_3$ layers ($|R_s^{\mathrm{SRO}} M^{\mathrm{SRO}}| > |R_s^{\mathrm{LSMO}} M^{\mathrm{LSMO}}|$), the sign reversal of ρ_{yx} is observed around ±3 T at 100 and 75 K, as shown in Fig. 3(a).

As T decreases from 75 to 50 K, the hysteresis loops observed in the Hall resistivity (ρ_{yx}) and magnetization (M) curves become wider, as shown in Figs. 4(a) and 4(b). At 50 K, the magnetization process is similar to that at 75 K [compare Figs. 3(b) and 4(b)], and a sign change in ρ_{yx} around ±3 T is also observed [Fig. 4(a)]. With a further decrease in T from 50 K, however, the overall H dependence of ρ_{yx} becomes quite different from that above 50 K. As shown in Fig. 4(c), the hysteresis loops in ρ_{yx} merge at 10 K, and one large hysteresis loop appears. The magnitude of the hysteresis loop is as large as 10 T, which is much larger than that observed in $La_{0.67}Sr_{0.33}MnO_3$ and $SrRuO_3$ single-component systems [2–12]. Even if the strong demagnetization field for $La_{0.67}Sr_{0.33}MnO_3$ layers, ∼1 T obtained at 150 K and 200 K in Fig. 3(a), is taken into account, the magnitude of the hysteresis loop at 10 K is estimated to still be over 8 T.

At 10 K, as shown in Fig. 4(d), an inverted hysteresis is observed in the isothermal magnetization curve [25], which is not observed at high temperatures above 50 K [see Figs. 3(b) and 4(b)]. The inverted hysteresis observed at 10 K [Fig. 4(d)] means that the magnetization of the $La_{0.67}Sr_{0.33}MnO_3$ layers points in the opposite direction to the external magnetic field

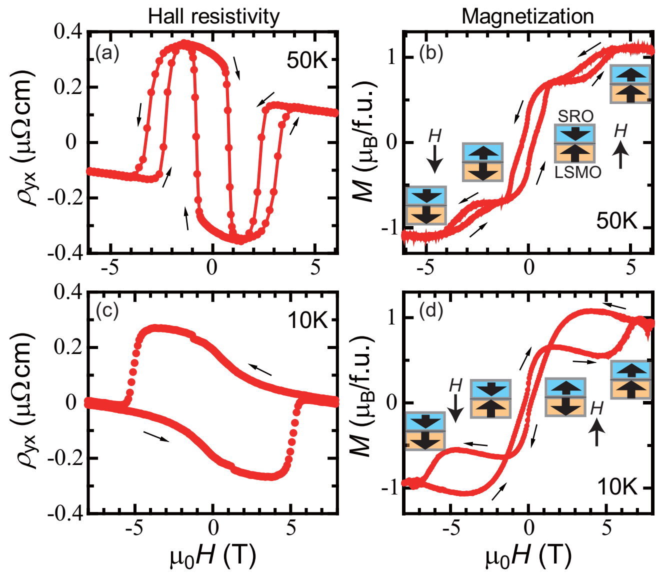

FIG. 4. (Color online) Magnetic-field (H) dependence of (a),(c) Hall resistivity (ρ_{yx}) and (b),(d) magnetization (M) for a $La_{0.67}Sr_{0.33}MnO_3|SrRuO_3$ superlattice sample at 50 K [(a) and (b)] and 10 K [(c) and (d)]. In (b) and (d), the diamagnetic contribution of the $SrTiO_3$ substrate was subtracted from the raw data. As for the magnetization data at 10 K shown in (d), see also Ref. [25].

($M^{\mathrm{LSMO}} < 0$ and $M^{\mathrm{SRO}} > 0$ in $H > 0$) in a low-H range at 10 K. At high T's, the magnetization of the $SrRuO_3$ layers tends to flip in a low-H range ($M^{\mathrm{LSMO}} > 0$ and $M^{\mathrm{SRO}} < 0$ in $H > 0$), because the net positive magnetization ($M^{\mathrm{LSMO}} + M^{\mathrm{SRO}} > 0$) is favorable for the energy gain of the Zeeman effect. By contrast, owing to an additional energy gain related to the perpendicular magnetic anisotropy of $SrRuO_3$ layers which develops at low T's [26], the inverted hysteresis loop is stabilized at 10 K [20]. The antiferromagnetically coupled magnetization of the $La_{0.67}Sr_{0.33}MnO_3$ layers ($M^{\mathrm{LSMO}} < 0$ in $H > 0$) induces a positive anomalous Hall resistivity in a positive H; this sign is the same as that of anomalous Hall resistivity for the $SrRuO_3$ layers. Hence, multiple hysteresis loops merge and one large hysteresis loop appears in the Hall resistivity of the superlattice sample at 10 K, as shown in Fig. 4(c). Because of the strong antiferromagnetic coupling in our superlattice samples, the magnitude of the hysteresis loop becomes larger than 8 T; such a large hysteresis has not been achieved in other perovskite-oxide superlattices [27].

IV. CONCLUSION

In conclusion, we measured the anomalous Hall effect for $La_{0.67}Sr_{0.33}MnO_3|SrRuO_3$ superlattices. The anomalous Hall effect in $La_{0.67}Sr_{0.33}MnO_3$ layers appears below 300 K, while that in $SrRuO_3$ layers appears below 100 K. The anomalous Hall effect in the superlattices is well explained by a sum of anomalous Hall resistivities of $La_{0.67}Sr_{0.33}MnO_3$ and $SrRuO_3$ layers, regardless of the antiferromagnetic coupling between the $La_{0.67}Sr_{0.33}MnO_3$ and $SrRuO_3$ layers below 110 K. Since the signs of the anomalous Hall coefficients are different between the $La_{0.67}Sr_{0.33}MnO_3$ and $SrRuO_3$ layers, and since the magnetization directions of the $La_{0.67}Sr_{0.33}MnO_3$ and $SrRuO_3$ layers are opposite to each other in a low-H range due to anitiferromagnetic interlayer coupling, the Hall resistivity in the $La_{0.67}Sr_{0.33}MnO_3|SrRuO_3$ superlattices shows a nonmonotonic magnetic-field dependence. Especially at 10 K, multiple hysteresis loops merge to form one hysteresis loop that is wider than 8 T in the Hall resistivity. In many cases, hysteresis in anomalous Hall resistivity results from magnetic anisotropies in materials; for ferromagnetic materials with a large anisotropy, the anomalous Hall resistivity often shows a large hysteresis loop. In the present $La_{0.67}Sr_{0.33}MnO_3|SrRuO_3$ superlattices, by contrast, the large hysteresis loop is produced by magnetic competition among the antiferromagnetic interlayer coupling, the Zeeman effect, and magnetic anisotropies.

ACKNOWLEDGMENTS

We thank M. Kawasaki and A. Sawa for experimental help and S. Ito from Analytical Research Core for Advanced Materials, Institute for Materials Research, Tohoku University, for performing transmission electron microscopy on our samples. T.K. is supported by the Japan Society for the Promotion of Science JSPS through a research fellowship for young scientists. This work was supported by CREST "Creation of Nanosystems with Novel Functions through Process Integration" from JST, Japan, and Grants-in-Aid for Scientific Research on Innovative Areas "Nano Spin Conversion Science" (No. 26103005), Challenging Exploratory Research (No. 26610091), and Scientific Research (A) (No. 24244051) from MEXT, Japan.

[1] N. Nagaosa, J. Sinova, S. Onoda, A. H. MacDonald, and N. P. Ong, Rev. Mod. Phys. **82**, 1539 (2010).
[2] Y. Lyanda-Geller, S. H. Chun, M. B. Salamon, P. M. Goldbart, P. D. Han, Y. Tomioka, A. Asamitsu, and Y. Tokura, Phys. Rev. B **63**, 184426 (2001).
[3] S. C. Gausepohl, M. Lee, R. A. Rao, and C. B. Eom, Phys. Rev. B **54**, 8996 (1996).
[4] G. Cao, S. McCall, M. Shepard, J. E. Crow, and R. P. Guertin, Phys. Rev. B **56**, 321 (1997).
[5] Z. Fang, N. Nagaosa, K. S. Takahashi, A. Asamitsu, R. Mathieu, T. Ogasawara, H. Yamada, M. Kawasaki, Y. Tokura, and K. Terakura, Science **302**, 92 (2003).
[6] R. Mathieu, A. Asamitsu, H. Yamada, K. S. Takahashi, M. Kawasaki, Z. Fang, N. Nagaosa, and Y. Tokura, Phys. Rev. Lett. **93**, 016602 (2004).
[7] R. Mathieu, C. U. Jung, H. Yamada, A. Asamitsu, M. Kawasaki, and Y. Tokura, Phys. Rev. B **72**, 064436 (2005).
[8] P. Khalifah, I. Ohkubo, B. C. Sales, H. M. Christen, D. Mandrus, and J. Cerne, Phys. Rev. B **76**, 054404 (2007).
[9] N. Haham, Y. Shperber, M. Schultz, N. Naftalis, E. Shimshoni, J. W. Reiner, and L. Klein, Phys. Rev. B **84**, 174439 (2011).
[10] N. Haham, J. W. Reiner, and L. Klein, Phys. Rev. B **86**, 144414 (2012).
[11] F. Bern, M. Ziese, K. Dorr, A. Herklotz, and I. Vrejoiu, Phys. Status Solidi RRL **7**, 204 (2012).
[12] S. Shimizu, K. S. Takahashi, M. Kubota, M. Kawasaki, Y. Tokura, and Y. Iwasa, Appl. Phys. Lett. **105**, 163509 (2014).
[13] M. Ziese, I. Vrejoiu, E. Pippel, P. Esquinazi, D. Hesse, C. Etz, J. Henk, A. Ernst, I. V. Maznichenko, W. Hergert, and I. Mertig, Phys. Rev. Lett. **104**, 167203 (2010).
[14] Y. Lee, B. Caes, and B. N. Harmon, J. Alloys Compd. **450**, 1 (2008).
[15] X. Ke, M. S. Rzchowski, L. J. Belenky, and C. B. Eom, Appl. Phys. Lett. **84**, 5458 (2004).
[16] Q. Zhang, S. Thota, F. Guillou, P. Padhan, V. Hardy, A. Wahl, and W. Prellier, J. Phys.: Condens. Matter **23**, 052201 (2011).
[17] P. Padhan and W. Prellier, Appl. Phys. Lett. **99**, 263108 (2011).
[18] J.-H. Kim, I. Vrejoiu, Y. Khaydukov, T. Keller, J. Stahn, A. Rühm, D. K. Satapathy, V. Hinkov, and B. Keimer, Phys. Rev. B **86**, 180402(R) (2012).
[19] X. Ke, L. J. Belenky, V. Lauter, H. Ambaye, C. W. Bark, C. B. Eom, and M. S. Rzchowski, Phys. Rev. Lett. **110**, 237201 (2013).
[20] M. Ziese, I. Vrejoiu, and D. Hesse, Appl. Phys. Lett. **97**, 052504 (2010).
[21] S. Das, A. Herklotz, E. Pippel, E. J. Guo, D. Rata, and K. Dörr, Phys. Rev. B **91**, 134405 (2015).
[22] Y. Shiomi, Y. Handa, T. Kikkawa, and E. Saitoh, Appl. Phys. Lett. **106**, 232403 (2015).
[23] M. Ziese, F. Bern, A. Setzer, E. Pippel, D. Hesse, and I. Vrejoiu, Eur. Phys. J. B **86**, 42 (2013).
[24] W. J. Xu, B. Zhang, Z. X. Liu, Z. Wang, W. Li, Z. B. Wu, R. H. Yu, and X. X. Zhang, Europhys. Lett. **90**, 27004 (2010).
[25] It is noted that the magnitude of the magnetization at 4 T is larger than that at 8 T in Fig. 4(d), although the magnetizations of the $La_{0.67}Sr_{0.33}MnO_3$ and $SrRuO_3$ layers are ferromagnetically aligned along the magnetic-field direction at 8 T but not at 4 T. The decrease in magnetization above 4 T observed in Fig. 4(d) is probably an artifact which originates in an imperfect subtraction of the substrate magnetization.
[26] L. Klein, J. S. Dodge, T. H. Geballe, A. Kapitulnik, A. F. Marshall, L. Antognazza, and K. Char, Appl. Phys. Lett. **66**, 2427 (1995).
[27] M. Ziese, F. Bern, E. Pippel, D. Hesse, and I. Vrejoiu, Nano Lett. **12**, 4276 (2012).